Two-dimensional spatial optical solitons in bulk Kerr media stabilized by self-induced multiphoton ionization: Variational approach

S. Henz and J. Herrmann
Max-Born-Institut für Nichtlineare Optik und Kurzzeitspektroskopie, Rudower Chaussee 6, D-12474 Berlin, Germany
(Received 25 July 1995)

The beam parameters of spatial two-dimensional solitons in a bulk medium under the influence of the combined effects of diffraction, Kerr nonlinearity, and nonlinear index change by plasma creation will be studied with the help of a variational approach. A simple analytical relation for the power of a spatial two-dimensional soliton is derived which shows a two-valued behavior in dependence on the beam diameter. The variational approximation is compared with numerical and experimental results. The solution is proven to be stable against small perturbations in the whole parameter region.

PACS number(s): 42.65.Tg

Bright spatial solitons are self-trapped beams in a material where the diffraction is balanced by a nonlinear index change. In a pure Kerr-medium stable self-trapping is only possible for two-dimensional geometries as, for example, in planar waveguides, limiting the diffraction to one spatial direction [1]. In this case the obtained basic equation (nonlinear Schrödinger equation) and the physical properties for timelike solitons in fibers are completely analogous to that of a spatial soliton in $1+1$ dimensions. For a bulk medium the stationary solitary wave solution of the multidimensional extension of the cubic nonlinear Schrödinger equation is extremely unstable against propagation [2]. This instability is catastrophic in the sense that if the incident beam power exceeds the critical power transverse fluctuations can suffer a rapid expansion and the beam breaks up into a random pattern of several filaments [3]. However, this pessimistic conclusion concerning the possibility of realizing stable spatial solitary waves in $2+1$ dimensions in a bulk medium does not exclude the generation of multidimensional solitons under other physical conditions, this possibility is a promising topic of investigations with attractive applications. Recently it has been reported on some attempts of theoretical as well as experimental investigations of two-dimensional spatial solitons. For an extreme high-power laser pulse in the order of the 10 TW relativistic self-channeling in an underdense plasma has been predicted [4] and also lately experimentally demonstrated over a plasma length of 3 mm [5]. In such an extreme high-power region nearly all neutral molecules of the medium are ionized and relativistic self-focusing develops from an increase of electron inertia under the influence of the intense electromagnetic wave. For a lower power in the nonrelativistic region recently the self-channeling of a small-scale filament formed from a high-peak power femtosecond laser pulse of about 20 GW over a distance of 20 m in air has been observed in Ref. [6]. In this region of laser power only a portion of the molecules is ionized by the laser pulse and the Kerr nonlinearity of the neutral molecules is the reason for self-focusing, whereas the additional self-defocusing nonlinear index change by the self-induced photonionization leads to a counteracting which stabilizes the beam for a certain spot size. Spatial solitary waves with a much lower power in the order of μW has been predicted and observed [7] in photorefractive media, where the refractive index change of the medium is associated with the light-induced nonuniform screening of an external field or with the photovoltaic current.

In the present paper we investigate the evolution of an optical high-power beam in a Kerr medium under the influence of self-induced multiphoton ionization and analyze the possible existence of two-dimensional spatial solitons generated by the combined effects of Kerr nonlinearity and nonlinear index change by self-induced ionization. By the counteracting self-defocusing effect of the photoionized free electrons the unbounded growth of the Kerr nonlinearity is restricted. Under such conditions the beam breakup into filaments due to self-focusing is prevented and under certain conditions a stabilized multidimensional soliton can exist.

We start by deriving the nonlinear wave equation which describes the beam propagation of an intense optical pulse in a bulk Kerr medium under the influence of multiphoton ionization. In order to obtain an analytical expression we use the variational approach based on a suitable choice of a trial function for the radial dependence of the electric field envelope $E=1/2[A(r,t)\exp(i\omega_0 t-kz)+\text{c.c.}]$. The variational procedure leads to a system of ordinary differential equations for the beam parameters which are analogous to a one-dimensional movement of a mechanical particle in a given potential $U(y)$. The solution of these equations shows in general periodical changes of the radius, the curvature, and the intensity of the beam in dependence on the axial coordinate z. Special emphasis is laid on the possibility of self-trapped beams or two-dimensional spatial solitons with beam parameters not changing during the propagation. A simple analytical formula describing the relation between the power and the beam radius for a spatial soliton is derived which is analogous to the relation for a timelike soliton in fibers between the soliton power and the pulse duration. The soliton power in dependence on the beam radius shows a two valued behavior similar to the timelike solitons in a medium with saturable nonlinearity [8]. The analytical results will be compared with an exact numerical integration. Further on the stability of the spatial soliton against small fluctuations will be analyzed and both solution branches will be proven to be stable.

The refraction index change by the Kerr effect and the self-induced ionization can be described by the relation

$$\Delta n = n_2|A|^2 - \frac{1}{2}\frac{1}{n_0}\frac{N_e}{N_{\text{cr}}}, \tag{1}$$

where A is the slowly varying amplitude of the electric field strength, n_0 the linear refractive index, n_2 is the nonlinear coefficient due to the Kerr effect, $N_{\text{cr}}=(m\omega_0^2\epsilon_0)/e^2$ the critical plasma density, and N_e the number density of free electrons. Multiphoton and tunneling ionization are two limiting cases of optical-field induced ionization [9] and are often distinguished by using the Keldysh parameter $\Gamma=(I_i/W_q)^{1/2}$, where I_i is the ionization energy and W_q the free electron quiver energy. In the following we consider the case $\Gamma>1$, where multiphoton ionization dominates compared with the tunneling ionization and neglect secondary ionization by free electrons. The electron density is then given by

$$N_e = Na\int_{-\infty}^{t} |A(z,r,t')|^{2n}dt', \tag{2}$$

where n is the number of quanta necessary to ionize the molecules ($n\hbar\omega_0 \geqslant I_i$), N the number density of molecules, and $a=\omega_0 n^{1.5}[\epsilon_0/(8N_{\text{cr}}I_i)]^n$. The spatial and temporal dynamics of a pulse in a bulk Kerr medium under the influence of self-induced ionization are determined by the competitive interaction of diffraction, self-ionization, and self-defocusing by the multiphoton ionization. The reduced Maxwell equation for the slowly varying amplitude A then with (1) and (2) has the form

$$2ik\frac{\partial A}{\partial z} - \frac{1}{r}\frac{\partial}{\partial r}\left(r\frac{\partial A}{\partial r}\right) - 2k\kappa|A|^2A + \rho a A\int_{-\infty}^{\eta}|A(t')|^{2n}dt' = 0, \tag{3}$$

where r is the radial coordinate, z the longitudinal coordinate, k the linear wave number, $\eta=t-(z/v)$ the time of the moving frame of the pulse maximum, $\kappa=kn_2/n_0$, and $\rho=(k^2N)/(n_0^2N_{\text{cr}})$. We solve approximately Eq. (3) by means of the variational approach [10] based on a suitable choice of a trial function. In Eq. (3) we have restricted our analysis to the condition when the relaxation time of the Kerr effect and the group velocity dispersion can be neglected, while the time η appears just as a parameter. For air parameters the group velocity dispersion parameter is $k''=1.8\times10^{-29}$ (s^2/m) and consequently the dispersion length of a 200 fs pulse is about 2.2 km. However note that the critical physical time scale which determines the influence of dispersion is given by the rise time of the pulse shape and not by the pulse duration. As we will see later in the framework of our model after nonlinear propagation a nearly rectangular pulse shape with a very short rise time arises. Group velocity dispersion with $k''>0$ combined with a self-focusing Kerr contribution to the refractive index even would enforce the formation of a nearly rectangular shape (as in a fiber-grating compression), but the counteraction of the self-defocusing plasma contribution could remove such a shape. The same is true for the relaxation time of the Kerr effect as well as for dispersion of the plasma generated by light. For the solution of Eq. (3) the time dependence of the beam can be taken into account by the ansatz

$$A(z,r,\eta)=B(z,r)T(\eta), \tag{4}$$

where $T(\eta)$ is the normalized input shape. With ansatz (4) the Lagrangian for Eq. (3) becomes

$$L=-ik\left(B\frac{\partial B^*}{\partial z} - B^*\frac{\partial B}{\partial z}\right)T + \left|\frac{\partial B}{\partial r}\right|^2 T - k\kappa|B|^4T^3 + \frac{\rho}{n+1}|B|^{2n+2}aTg(\eta), \tag{5}$$

with $g(\eta)=\int_{-\infty}^{\eta}T^{2n}(t)dt$. To find a solution for Eq. (3) now is equivalent to the variational procedure

$$\delta\int_0^\infty rL\,dr=0. \tag{6}$$

For the solution of the variational problem (6) we use a Gaussian beam ansatz

$$B(z,r)=C(z)\exp\left(-\frac{r^2}{w^2(z)}+ib(z)r^2+i\Phi(z)\right), \tag{7}$$

where the maximum amplitude $C(z)$, the beam radius $w(z)$, the curvature parameter $b(z)$, and the phase $\Phi(z)$ are functions of z. Using (7) the integration in (6) can be done explicitly with respect to the radial variable r which yields

$$\mathscr{L}=\int_0^\infty Lrdr=-\frac{1}{4}kw^4C^2\frac{db}{dz}T-\frac{1}{2}kw^2C^2\frac{d\Phi}{dz}T + \frac{1}{2}C^2T+\frac{1}{2}b^2w^4C^2T-\frac{1}{8}k\kappa w^2C^4T^3 + \frac{1}{4}\frac{\rho}{(n+1)^2}w^2C^{2n+2}aTg(\eta). \tag{8}$$

The variation of the reduced Lagrangian (8) with respect to Φ, b, C, and w gives the following system of ordinary differential equations:

$$\frac{d}{dz}(w^2C^2)=0, \tag{9}$$

$$\frac{dw}{dz}=-\frac{2}{k}wb, \tag{10}$$

$$\frac{db}{dz}=-\frac{2}{k}\frac{1}{w^4}+\frac{2}{k}b^2+\frac{\kappa}{2w^2}C^2T^2 - \frac{n}{(n+1)^2}\frac{\rho}{kw^2}C^{2n}ag(\eta), \tag{11}$$

$$\frac{d\Phi}{dz}=\frac{2}{k}\frac{1}{w^2}-\frac{3}{4}\kappa C^2T^2+\frac{2n+1}{2(n+1)^2}\frac{\rho}{k}C^{2n}ag(\eta). \tag{12}$$

The relation (9) implies the conservation of the power $P(z)\equiv P_0=(\pi/4)\epsilon_0 cn_0w^2C^2T^2(\eta)$. Since (8) does not explicitly depend on the variable z the Hamiltonian $H=H_0$ is a second constant of motion:

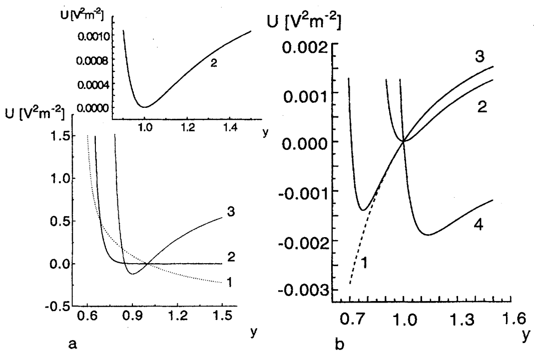

FIG. 1. Potential U in dependence on the normalized beam radius y. The parameters in (a) are $\gamma=2.725\times10^{-4}$. Curve 1: $P_0/P_{cr}=0.8$; curve 2: $P_0/P_{cr}=1.0014$; curve 3: $P_0/P_{cr}=1.5$. The parameters in (b) are $P_0/P_{cr}=1.0014$. Curve 1: $\gamma=0$; curve 2: $\gamma=2.725\times10^{-4}$; curve 3: $\gamma=2.725\times10^{-6}$; curve 4: $\gamma=2.725\times10^{-3}$.

$$H=-\frac{1}{2}C^2T-\frac{1}{2}b^2w^4C^2T+\frac{1}{8}k\kappa w^2C^4T^3 -\frac{1}{4}\frac{\rho}{(n+1)^2}w^2C^{2n+2}aTg(\eta). \quad (13)$$

Using (9) and (10) we obtain from (13) with the normalized variable $\zeta=z/(kw_0^2)$ for the relative beam radius $y=w(z)/w_0$

$$\frac{1}{2}\left(\frac{dy}{d\zeta}\right)^2=-\left[\left(\frac{1}{y^2}-1\right)\left(2-2\frac{P_0}{P_{cr}}\right)+\left(\frac{1}{y^{2n}}-1\right)\gamma\left(\frac{P_0}{P_{cr}}\right)^n -2b_0^2w_0^4\right]\equiv-U(y). \quad (14)$$

Here $w_0=w(z=0)$, $b_0=b(z=0)$, $P_0=P(z=0)$ are the input parameters at $z=0$, λ is the wavelength, $P_{cr}=\pi[n_0^2/(n_2k^2)]\epsilon_0c$ is the critical power of self-focusing [3], and

$$\gamma=\frac{1}{2^{n-3}}\frac{n^{1.5}}{(n+1)^2}\frac{c}{n_0^nw_0^{2n-2}}\left(\frac{\pi}{\lambda}\right)^3\frac{N}{N_{cr}}\left(\frac{P_{cr}}{\pi cI_iN_{cr}}\right)^n\frac{g(\eta)}{T^{2n}(\eta)}. \quad (15)$$

With the solution $y(z)$ we find from relation (10) the curvature parameter $b(z)$ and from the conservation of the power the amplitude $C(z)$. With the help of the variational approach the nonlinear wave propagation has been reduced to an analogue of a simple one-dimensional mechanical problem with a potential $U(y)$, where the particle's coordinate is related to the beam radius w, the particle's velocity corresponding to Eq. (10) to the curvature parameter b, and the time to the axial coordinate z. In Fig. 1(a) the potential $U(y)$ is depicted for air parameters under normal conditions with $n_2=7.4\times10^{-26}(m^2/V^2)$, $n_0=1.0$, $P_{cr}=1.82$ GW, $I_i=14.54$ eV, $n=10$ and the laser parameters $\lambda=800$ nm, $w_0=52.6$ μm, and $b_0=0$ for the maximum of the input pulse ($\eta=0$), a shape function $T(\eta)=\text{sech}(1.76\eta/\tau_0)$, width $\tau_0=200$ fs, and for the three different input pulse powers P_0/P_{cr}. For a power $P_0/P_{cr}=0.8$ below the critical one in curve 1 the potential decreases monotonously since the diffraction prevails over the self-focusing. A "particle" starting at $y=1$ falls monotonously or the beam radius y increases monotonously. In curve 3 for a power $P_0/P_{cr}=1.5$ larger than the critical power the predominance of the self-focusing results in a decreasing beam radius y because of the decreasing potential. As a consequence the intensity I increases and the ionization of the neutral molecules comes into play. The self-defocusing due to the plasma creation leads then finally again to an increase of the potential for $y<y_{min}$. The minimum of the potential, where both effects balance each other, can be determined from Eq. (14) and is given by

$$y_{min}=\left(\frac{n\gamma\left(\frac{P_0}{P_{cr}}\right)^n}{2\frac{P_0}{P_{cr}}-2}\right)^{1/(2n-2)}. \quad (16)$$

A minimum in the potential is a necessary condition for the existence of a spatial soliton or a self-trapped beam. The characteristic of a spatial soliton is the constance of the beam radius during the propagation and that the curvature parameter b is equal to zero. Consequently the potential has its minimum at $y=1$. Therefore we find from Eq. (16) the relation of a spatial soliton $P_0=P_s$

$$\frac{P_s}{P_{cr}}-1=\frac{1}{2}\gamma n\left(\frac{P_s}{P_{cr}}\right)^n. \quad (17)$$

For fixed material parameters and a fixed time, e.g., $\eta=0$, Eq. (17) represents a relation between the power and the beam radius w_0 (via the coefficient γ) analogous to the relation for the timelike solitons in fibers between the soliton peak power and the pulse duration. Curve 2 of Fig. 1(a) shows the potential for a power $P_0/P_{cr}=1.0014$ fulfilling the soliton relation (17) for $\eta=0$ and the other parameters given above. As seen in the enlarged inset in this case the potential $U(y)$ has its minimum at $y=1$ and therefore the "particle" rests in this point.

In Fig. 1(b) the potential is depicted for four different parameters γ for a fixed input power $P_0/P_{cr}=1.0014$. In curve 1 for $\gamma=0$ the potential decreases monotonously with decreasing y, i.e., the beam radius decreases, and the known catastrophic self-focusing appears [2,3], whereas in curve 2 and 3 due to a finite γ a minimum exists. Here curve 2 corresponds to the soliton relation in Eq. (17) with the minimum at $y=1$. The behavior of the potential for $\gamma=2.725\times10^{-3}$ is depicted in curve 4, which shows a minimum for $y>1$. In Fig. 2 the normalized beam radius y and the normalized curvature parameter b/w_0^2 are shown, respectively, as functions of the axial coordinate z obtained by solving (14), (10), and (11) with a Runge-Kutta method with adaptive stepsize control, where $C(z)$ is replaced by the power conservation. The parameters in the three curves are the same as in the corresponding curves of Fig. 1(a). As expected and in accordance with the potential curve for an input power $P_0/P_{cr}=0.8$ in curve 1 the beam radius increases monotonously during the propagation as a result of the predominance of the diffraction. In curve 2 of the same figure with $P_0/P_{cr}=1.0014$ the soliton condition is realized and consequently the beam radius does not change and the

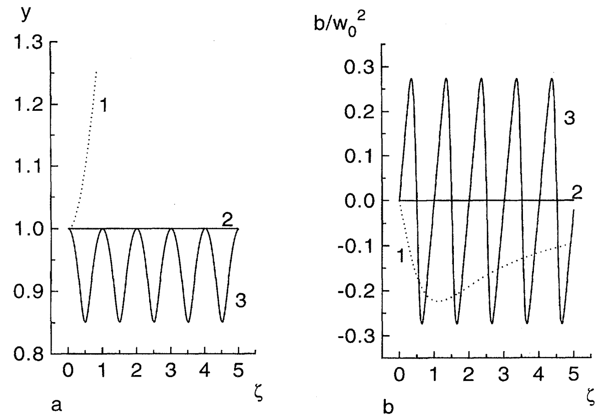

FIG. 2. Normalized beam radius (a) and normalized curvature parameter (b) in dependence on the normalized propagation distance ζ. Parameters as in Fig. 1(a).

curvature parameter vanishes. In curve 3 with $P_0/P_{\mathrm{cr}}=1.5$ the beam radius as well as the curvature parameter reveal an oscillating behavior around $y=1$ and $b/w_0^2=0$, respectively.

In Fig. 3(a) for the same parameters the normalized intensity $I=C^2T^2[(n_2k^2w_0^2)/(4n_0)]$ is shown. In curve 1 the intensity decreases during the propagation since the beam radius increases. In curve 2 for $P_{\mathrm{cr}}/P_0=1.0014$ which means that the soliton condition is fulfilled the intensity stays constant during the propagation and finally in curve 3 for $P_0/P_{\mathrm{cr}}=1.5$ we see similar oscillations for the beam radius and the curvature parameter as above.

In Fig. 3(b) for the same parameters as above the variation of the phase $\mathbf{\Phi}$ is depicted. For the soliton in curve 2 the phase $\mathbf{\Phi}$ shows a constant decrease $d\Phi/d\zeta=-\beta$, whereas for the other parameters in curve 1 and 3 the increase of $\mathbf{\Phi}$ depends on z.

Let us still discuss the properties of the three-dimensional soliton described by Eq. (17) more in detail and under more general conditions. For a given pulse duration and a fixed time (e.g., $\eta=0$) the normalized soliton power P_s/P_{cr} is just a function of the parameter γ depending on the beam radius w_0 and on the number n of the photons necessary for the

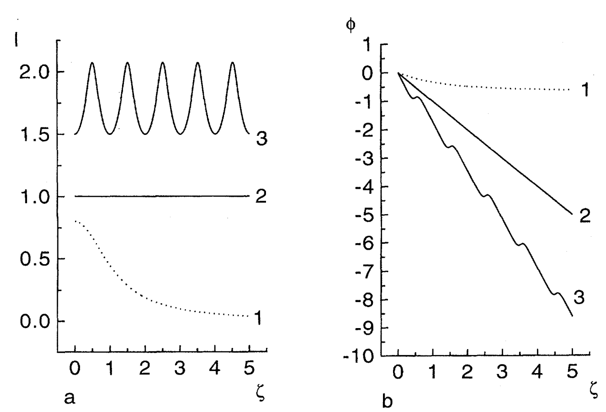

FIG. 3. Normalized intensity (a) and phase Φ (b) in dependence on the normalized propagation distance ζ. Parameters as in Fig. 1(a).

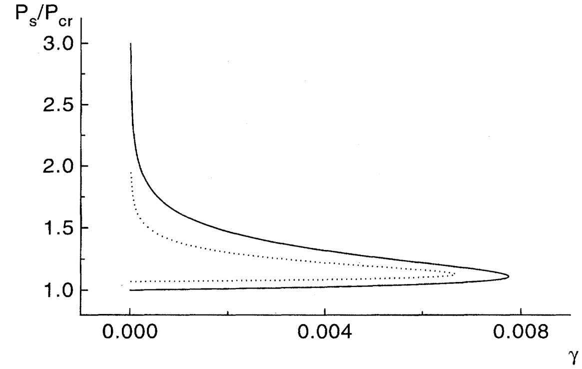

FIG. 4. Normalized soliton power in dependence on the parameter γ: analytical calculation (solid line) and numerical calculation (dotted line).

ionization of the molecules. In Fig. 4 in the solid lines the soliton power P_s/P_{cr} is plotted in dependence on the parameter γ. For small values of γ one gets a soliton power P_s/P_{cr} only slightly larger than unity. With increasing γ the soliton power becomes a two-valued function of γ. γ depends on the beam radius w_0 and consequently for the same beam radius two soliton states with different powers exist. For a value of γ larger than a critical one ($\gamma>\gamma_{\mathrm{cr}}$) no soliton solution exists. Using the soliton relation (17) this critical value can be estimated to

$$\gamma_{\mathrm{cr}}=\frac{2(n-1)^{n-1}}{n^{n+1}}. \tag{18}$$

The parameter γ_{cr} for a soliton is related with a minimum soliton beam radius, solitons with a smaller beam radius as given by (15) and (18) do not exist.

The two-valued behavior of the soliton states in Fig. 4 resembles the corresponding curves for the timelike solitons in fibers with saturable nonlinearity as considered in Ref. [8] for a type of nonlinearity $\Delta n=n_2|A|^2-n_4|A|^4$ or $\Delta n=(n_2|A|^2)/(1+\gamma|A|^2)$.

The analytical formula (17) illustrated in Fig. 4 represents the main result of the present paper and yields a simple description of the main property of solitary beams in the considered system. In order to prove how sensitive this result is depends on the used approximation with a fixed shape described by the trial function (7) we performed a numerical integration of Eq. (3). With the soliton ansatz $A=\exp(-i\beta z)\mathbf{\Psi}(r)$ from Eq. (3) an ordinary differential equation can be found for $\mathbf{\Psi}(r)$ which was solved numerically. The corresponding result for the soliton power in dependence on the parameter γ is depicted in the dotted line of Fig. 4. As seen the variational approach used in the present work yields qualitatively the same behavior and the quantitative deviation is only small compared with the exact numerical result. Therefore for the description of two-dimensional solitons in the considered physical system the variational approach can be considered as a reasonable approximation. Let us now examine the stability property of the soliton states in Fig. 4. Equation (3) belongs to a class of nonlinear evolution equations for which a stability criterium was derived in Refs. [11, 12]. Accordingly a necessary [11] and a sufficient [12] crite-

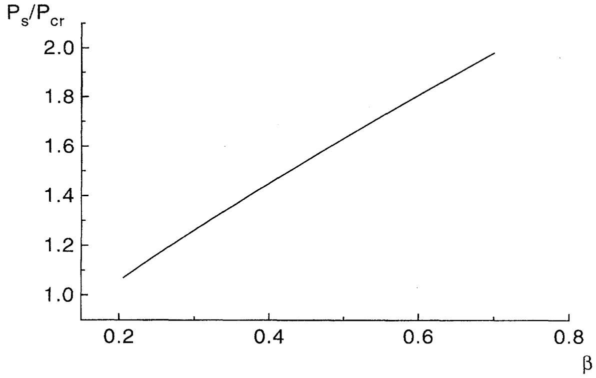

FIG. 5. Normalized soliton power in dependence on the wave number shift β. Since $dP_s/d\beta>0$ both soliton solution branches are stable.

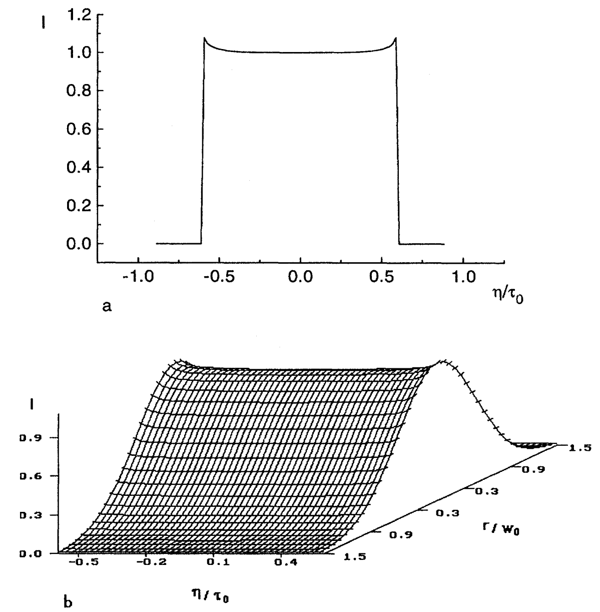

FIG. 6. Soliton shape on the axial axis (a) and three-dimensional plot of the normalized soliton intensity versus the time η and the radial variable r for a soliton beam radius w_0=52, 6 μm.

rion for the stability of the soliton states of Eq. (3) against small perturbations is the condition $(dP_s/d\beta)>0$, where P_s is the soliton power (17) and β is the wave number shift $(d\Phi/d\zeta)=-\beta$. The result of our numerical calculation for the function $P(\beta)$ is depicted in Fig. 5. As seen the function $P(\beta)$ shows a monotonously increase with β, therefore the soliton solution is stable in the whole parameter region. However note that the criterion $(dP/d\beta)>0$ for soliton stability in the case of the higher order nonlinearities ensures only stability against small perturbations and has to be distinguished from the stability against large perturbations [13]. For large perturbations as in the case of the collisions of two solitons which are stable against small perturbations for the different nonlinear models a variety of effects can be found reaching from an elastic collision behavior, i.e., stability against large perturbations (robust solitons) [13], a "quasisoliton" behavior which is accompanied by an appreciable radiative peak or background [14], or a fusion or alternatively a pulse splitting at collisions [15]. We must bear in mind that in our discussion we have mainly referred to a fixed time, as e.g., the time of the pulse maximum $\eta=0$, but the general time dependence of all relations is included in the input parameters $P_0(\eta)$ and $\gamma(\eta)$. However, the nonlinear refractive index change and the diffraction act in a different way on the various parts of the pulse leading to a narrowing of the pulse shape. Using the explicit time dependence of relation (17) in Fig. 6(a) the pulse shape $I(\eta)$ on the axis $r=0$ is depicted for a soliton beam radius w_0=52, 6 μm and with the other material parameters given above. As seen the two-dimensional soliton shows a nearly rectangular shape with a normalized intensity near unity. As mentioned at the beginning dispersion effects neglected in our analysis could remove such behavior. In our model the sharp cutoff of the shape is caused by the decrease of the input function $T(\eta)=\mathrm{sech}(1.76\eta/\tau_0)$ which corresponding to (15) yields an increase of the parameter $\gamma(\eta)$ on the pulse wings because the function $g(\eta)$ changes only slowly with time. Therefore at the pulse wings the parameter γ reaches the critical value of relation (18) with $\gamma_{cr}=7.748\times10^{-3}$. For the subcritical parts of the pulse the soliton relation (17) cannot be fulfilled and the pulse wings are suppressed by diffraction induced erosion. The small increase of the intensity near the edges of the shape in Fig. 6(a) is connected with the slight increase of the soliton peak power near the critical parameter γ_{cr} in Fig. 4. In Fig. 6(b) in a three-dimensional plot the normalized intensity versus the time η and the radial variable r for the soliton is illustrated where the radial shape here is described by the fixed Gaussian shape approximation used in the present approach.

Let us finally compare our theoretical results with the experimental observations in Ref. [6] where the self-channeling of a filament formed from an ultrashort laser pulse was reported. In the initial stage of propagation of about 10 m after a decrease of the beam diameter and an increase of the intensity a filament was formed with a diameter of about 80 μm and 0.75 mJ whose diameter remained constant during a propagation distance of about 20 m. The initial stage of the beam evolution as observed in [6] cannot be described by our theoretical results which predict a periodical change of the beam diameter or the intensity above the critical power. The main reason for the difference can be found in the application of the fixed-shape approximation in our approach. From the numerical study we found that a beam with an arbitrary initial shape and with a power somewhat larger than the soliton power will change its shape and power by diffraction erosion until the soliton condition is fulfilled. Then during the further propagation the beam parameters remain constant. This is in agreement with the experimental results where only a fraction of the initial radiation was trapped. However, the stable propagation and the parameters of the self-channeled filament agree rather well with our soliton relation in Eq. (17) for a two-dimensional spatial soliton in a Kerr medium stabilized by the refraction from the plasma created by the intense laser pulse.

In conclusion, with the help of the variational approach the evolution of a high-power beam under the influence of the combined effects of diffraction, Kerr nonlinearity, and refraction from the plasma created by multiphoton ionization by the intense laser pulse has been investigated. The conditions for the existence and the properties of two-dimensional spatial solitons have been derived and studied in detail and an analytical formula for the soliton power in depence on the beam radius has been derived. The power of the two-dimensional spatial soliton shows a two-valued behavior.

We gratefully acknowledge support by the Deutsche Forschungsgemeinschaft.

[1] V. E. Zakharov and A. B. Shabat, Zh. Eksp. Teor. Fiz. **61**, 118 (1971) [Sov. Phys. JETP **34**, 62 (1972)]; S. Maneuf, R. Desailly, and C. Froehly, Opt. Commun. **65**, 193 (1988); J. S. Aitchinson *et al.*, Opt. Lett. **15**, 471 (1990).
[2] J. Juul Rasmussen and K. Rypdal, Phys. Scr. **33**, 481 (1986).
[3] J. H. Marburger, Prog. Quantum Electron. **4**, 35 (1975).
[4] C. E. Max, J. Arons, and A. B. Langdon, Phys. Rev. Lett. **33**, 209 (1974); P. Sprangle, C. M. Tang, and E. Esarey, IEEE Trans. Plasma **PS-15**, 145 (1987); G. Z. Sun, E. Ott, Y. C. Lee, and P. Guzdar, Phys. Fluids **30**, 526 (1987); A. B. Borisov *et al.*, Phys. Rev. Lett. **65**, 1753 (1990).
[5] A. B. Borisov *et al.*, Phys. Rev. Lett. **68**, 2309 (1992); P. Monot *et al.*, *ibid.* **74**, 2953 (1995).
[6] A. Braun *et al.*, Opt. Lett. **20**, 73 (1995).
[7] M. Segev, B. Crosignani, A. Yariv, and B. Fischer, Phys. Rev. Lett. **68**, 923 (1992); G. Duree *et al.*, *ibid.* **71**, 533 (1993); M. Segev *et al.*, *ibid.* **73**, 3211 (9994); M. F. Shih *et al.*, Electr. Lett. **31**, 826 (1995).
[8] S. Gatz and J. Herrmann, J. Opt. Soc. Am. **11**, 2296 (1991); J. Herrmann, Opt. Commun. **87**, 161 (1992).
[9] L. V. Keldysh, Zh. Eksp. Teor. Fiz. **47**, 1945 (1964) [Sov. Phys. JETP **20**, 1307 (1965)].
[10] D. Anderson, Phys. Rev. A **27**, 3135 (1983); M. Karlson, D. Anderson, M. Desaix, and M. Lisak, Opt. Lett. **13**, 1373 (1991); J. Herrmann, J. Opt. Soc. Am. B **8**, 1507 (1991).
[11] N. G. Vakhitov and A. A. Kolokov, Radiophys. Quantum Electron. **16**, 783 (1975).
[12] E. W. Laedke, K. H. Spatschek, and L. J. Stenflo, J. Math. Phys. **24**, 2764 (1987).
[13] A. E. Kaplan, Phys. Rev. Lett. **55**, 1291 (1985); R. H. Enns, S. S. Rangnekar, and A. E. Kaplan, Phys. Rev. A **35**, 466 (1987); *ibid.* **36**, 1270 (1987).
[14] S. Cowan, R. H. Enns, S. S. Rangnekar, and S. S. Sanghera, Can. J. Phys. **64**, 311 (1986).
[15] S. Gatz and J. Herrmann, IEEE J. Quantum Electron. **28**, 1232 (1992).